Vacuum polarization and stress-energy of a quantum field inside of two-dimensional black holes

Paul R. Anderson* and Amanda Peake

Department of Physics, Wake Forest University, Winston-Salem, North Carolina, 27109, USA

Shohreh Gholizadeh Siahmazgi†

Department of Mathematics, Wake Forest University, Winston-Salem, North Carolina, 27109, USA and Department of Physics, Wake Forest University, Winston-Salem, North Carolina, 27109, USA

(Received 31 October 2025; accepted 13 April 2026; published 25 June 2026)

Quantum effects are studied in both Schwarzschild spacetime and a spacetime in which a null shell collapses to form a black hole via the vacuum polarization $\langle\phi^2\rangle$ and stress-energy tensor $\langle T_{ab}\rangle$ for a massless minimally coupled scalar field in two dimensions. For Schwarzschild spacetime, the focus is on the Boulware and Unruh states. For the collapsing null shell spacetime, the *in* vacuum state is used. Instabilities of the Unruh and *in* states resulting from the behavior of $\langle\phi^2\rangle$ in the regions inside and outside of the horizon are found. The question of how well the Unruh state for the eternal black hole approximates quantum effects in the interior of a black hole that forms from collapse is addressed.

DOI: 10.1103/dfcd-93tb

I. INTRODUCTION

Two important states for eternal black holes are the Boulware state [1] and the Unruh state [2]. The Boulware state is the true vacuum state at both past and future null infinity. It is well suited to describe the vacuum state outside of a spherically symmetric star. However, the stress energy of a quantum field diverges on the past and future horizons in this state. The Unruh state is the best state to approximate Hawking radiation for an eternal black hole. The stress energy is finite on the future horizon, and there is a flux of radiation in a thermal distribution at the Hawking temperature going out to future null infinity. The stress energy does diverge on the past horizon for the Unruh state, but this is not important because there is no past horizon for a black hole that forms from collapse. For a black hole that forms from collapse in a spherically symmetric, asymptotically flat spacetime, the *in* state is defined to be the vacuum state at past null infinity along with the condition that before the black hole forms the mode functions are regular at $r = 0$.

While these states have been studied extensively in both two dimensions, 2D, and four dimensions, 4D, most of what is known about them for Schwarzschild black holes is for the region outside the past and future horizons which we call the exterior region and for the horizons that bound that region. In this paper, we work with a massless minimally coupled scalar field in 2D where analytic calculations are possible and investigate the behaviors of the vacuum polarization $\langle\phi^2\rangle$ and the stress-energy tensor $\langle T_{ab}\rangle$ in Schwarzschild spacetime. For the stress-energy tensor, the focus is on the region inside the future horizon and outside the past horizon which we call the interior region.

The vacuum polarization does not appear to have been studied previously in any 2D black hole spacetime. Previous calculations of the stress-energy tensor for a massless minimally coupled scalar field in 2D Schwarzschild spacetime for these states and the Hartle-Hawking state [3] have been done, and the results have been analyzed in the exterior region [4–7], but not in the interior region with the exception of correlations between the energy density in the interior and exterior regions [8]. The stress-energy tensor was also computed and analyzed in the interior (and exterior) for the case of dust collapsing to form a black hole in 2D [9]. There have been several full numerical calculations of the vacuum polarization [10–14] and the stress-energy tensor [15–24] for scalar fields in Schwarzschild spacetime in the Boulware, Unruh, and Hartle-Hawking states in the exterior region. There have been two full numerical calculations of the vacuum polarization in part of the interior region of Schwarzschild spacetime in 4D in the Hartle-Hawking and Unruh states [25,26]. Recently there has been a calculation of the vacuum polarization and one component of the stress-energy tensor near the trajectory of a massless spherically symmetric shell in 4D that collapses to form a black hole [27].

One reason it is interesting to investigate the behavior of the vacuum polarization is that it was previously found that, for a massless minimally coupled scalar field in the Unruh

*Contact author: anderson@wfu.edu
†Contact author: gholizs@wfu.edu

state, the symmetric two-point function or Hadamard Green's function grows without bound in time at late times in the static region outside of an eternal 2D black hole when the points are split in the radial direction [28]. The vacuum polarization can be used to test the robustness of the previous result since it is a function of just one spacetime point, so there is no ambiguity associated with the way in which the points are split.

The existence of the linear growth in time of the two-point function appears to be indicative of some type of instability associated with the Unruh state. There is also evidence that it is associated with an infrared divergence in the two-point function which is caused by infrared divergences in the mode functions [29]. There is an interesting exception which is the collapsing null shell spacetime in two dimensions. For the model studied in [28] the mode functions consist of differences between two solutions to the mode equation that both have infrared divergences; however these divergences cancel. Nevertheless, at late times the same linear growth appears to leading order as was found for the Unruh state. There is also a subleading term which grows logarithmically in time and is not present for the Unruh state. In 4D one would expect the linear growth to occur in spacetimes where scattering effects do not remove the infrared divergence in the mode functions. Such growth has been found for a massless minimally coupled scalar field in the Unruh state in 4D Schwarzschild–de Sitter spacetime in the static region between the black hole and cosmological horizons [30].

In this paper, we find the same linear growth in time for the vacuum polarization that was found previously in [28], for the symmetric two-point function occurs in the exterior region of 2D Schwarzschild spactime and the region outside the shell and the horizon of a null shell that collapses to form a 2D black hole. We also extend previous calculations of the stress-energy tensor for all three states and the Hartle-Hawking state into the region inside the horizon. We compare both the vacuum polarization and the stress energy in the null shell spacetime in both the interior and exterior regions with those in Schwarzschild spacetime when the field is in the Unruh state. This has previously been done for the stress energy in the exterior region but not otherwise. The question of how good an approximation the Unruh state is to the *in* state is important because it is much easier in 4D to compute both the vacuum polarization and the stress-energy tensor for an eternal black hole than it is to compute them if the black hole forms from collapse.

In Sec. II, we give a brief overview of Schwarzschild spacetime and the relevant coordinates. In Sec. III, the complete sets of solutions to the mode equation that are used to define the Boulware, Unruh, and *in* states are given. In Sec. IV, the quantity $\langle\phi^2\rangle$ is computed and discussed for the Boulware, Unruh, and *in* states, and its behavior is investigated for each. A comparison is made between $\langle\phi^2\rangle$ for the Unruh and *in* states. In Sec. V the stress-energy tensor for the scalar field is analyzed for all four states in the interior region. Again a comparison is made of its behaviors for the Unruh state and the *in* state. Section VI contains a summary and discussion of our results. A derivation of the stress-energy tensor in both the interior and exterior regions for all four states is given in the Appendix. Throughout, we use units such that $\hbar = c = G = 1$.

II. SPACETIMES CONSIDERED HERE

A. Schwarzschild spacetime

One of the spacetimes we consider is a 2D Schwarzschild black hole with the line element

$$ds^2 = -f(r)dt^2 + \frac{dr^2}{f(r)}, \tag{2.1}$$

where $f(r) = 1 - \frac{2M}{r}$ and M represents the mass of the black hole. The tortoise coordinate is

$$r_* = \int^r \frac{dr'}{f(r')} = r + 2M \log\left|1 - \frac{r}{2M}\right|. \tag{2.2}$$

In the interior region, t is a space coordinate. Both $-r$ and r_* can serve as time coordinates because they increase as one goes from the horizon to the spacelike singularity at $r = 0$.

The Penrose diagram for Schwarzschild spacetime is given in Fig. 1.

It is useful to define left and right moving null coordinates u and v. For the interior and exterior regions,

$$u_{\rm int} = r_* - t, \tag{2.3a}$$

$$u_{\rm ext} = t - r_*, \tag{2.3b}$$

and in both regions,

$$v = r_* + t. \tag{2.3c}$$

Note that the coordinate v is regular on the future horizon while $u_{\rm ext} \to +\infty$ and $u_{\rm int} \to -\infty$ there. The coordinates $u_{\rm int}$ and $u_{\rm ext}$ are regular on the past horizon in the interior and exterior regions respectively while $v \to -\infty$ everywhere on the past horizon.

The right-moving null Kruskal coordinate in the interior and exterior regions is

$$U(u_{\rm int}) = 4Me^{\frac{u_{\rm int}}{4M}}, \tag{2.4a}$$

$$U(u_{\rm ext}) = -4Me^{-\frac{u_{\rm ext}}{4M}}, \tag{2.4b}$$

and the left-moving Kruskal coordinate in both regions is

$$V(v) = 4Me^{\frac{v}{4M}}. \tag{2.4c}$$

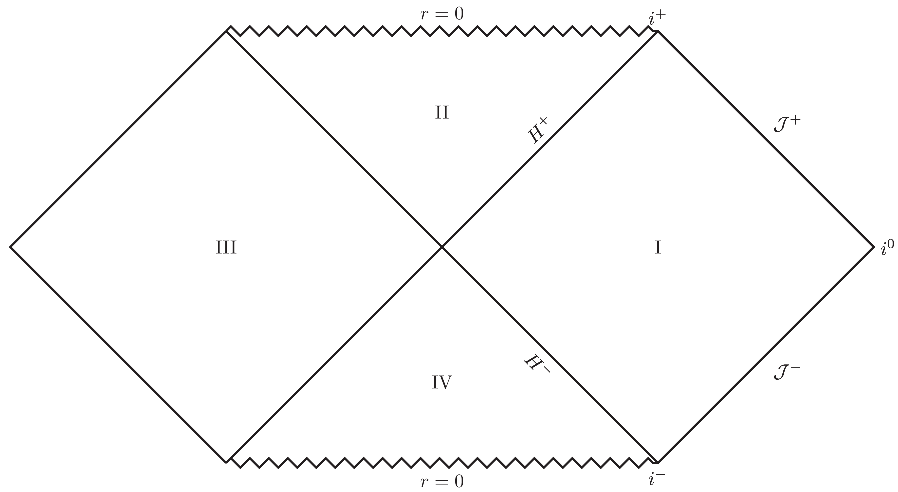

FIG. 1. Penrose diagram for a Schwarzschild black hole. The wavy lines are the singularities at $r = 0$. The future and past horizons are labeled $H^{\pm}$, and future and past null infinity are labeled $\mathscr{I}^{\pm}$. We call the region labeled I the exterior region and the region labeled II the interior region.

These coordinates are well behaved throughout the spacetime.

B. Collapsing null shell spacetime

We take the 2D analog of a 4D spherically symmetric massless shell that contracts along the null ray $v = v_0$ for any $-\infty < v_0 < \infty$. The metric inside the shell is the flat space metric given by

$$ds^2 = -dt_F^2 + dr^2. \tag{2.5}$$

In 2D one can have $-\infty < r < \infty$. However, to approximate the 4D case where $r \geq 0$ one can put a perfectly reflecting mirror at $r = 0$ and just consider the spacetime outside the mirror. That is what we do here.

In the flat space region inside the shell we define coordinates

$$u_F = t_F - r, \qquad v = t_F + r, \tag{2.6}$$

where t_F is the flat space time coordinate. The metric outside the shell is given by the Schwarzchild metric (2.1). The two metrics are matched along the shell trajectory, which is a null trajectory along $v = v_0$. The matching is set up so that the coordinates r and v are continuous across the trajectory, but t and u are not. In the region outside the shell and the horizon, we can write u_{ext} in terms of u_F by matching along the trajectory $v = v_0$. The result is [7]

$$u_{\text{ext}} = u_F - 4M \log\left(\frac{v_H - u_F}{4M}\right). \tag{2.7}$$

Inverting this gives [31]

$$u_F(u_{\text{ext}}) = v_H - 4MW\left[\exp\left(\frac{v_H - u_{\text{ext}}}{4M}\right)\right], \tag{2.8}$$

where $v_H = v_0 - 4M$ and W is the Lambert W function. Following the same process as above, we can use u_{int} as defined in Eq. (2.3a) in the region outside the shell and inside of the horizon with the result

$$u_{\text{int}} = -u_F + 4M \log\left(\frac{u_F - v_H}{4M}\right) \tag{2.9}$$

and

$$u_F(u_{\text{int}}) = v_H - 4MW\left[-\exp\left(\frac{u_{\text{int}} + v_H}{4M}\right)\right]. \tag{2.10}$$

These coordinates have the following properties:

(1) The event horizon of the black hole within the flat space region is at $u_F = v_H = v_0 - 4M$.

(2) The null shell trajectory reaches the singularity $r = 0$ at $u_F = v_0$. Therefore, the part of the trajectory in the interior region of the black hole is $v_H < u_F \leq v_0$.

The Penrose diagram for a black hole formed from a collapsing null shell is shown in Fig. 2.

III. MODE EQUATION

We consider a massless minimally coupled scalar field ϕ satisfying

$$\Box\phi = \frac{1}{\sqrt{-g}}\partial_\alpha(g^{\alpha\beta}\sqrt{-g}\partial_\beta)\phi = 0. \tag{3.1}$$

For the flat space metric (2.5), one finds

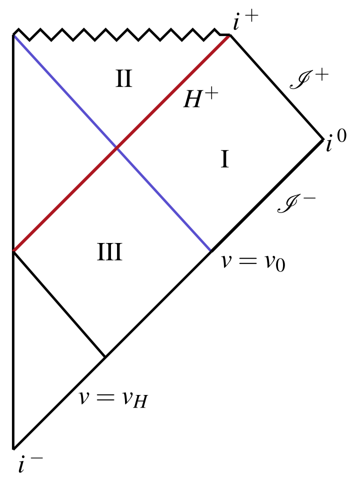

FIG. 2. Penrose diagram of a black hole that forms from a collapsing null shell in 4D or in 2D when a perfectly reflecting mirror is placed at $r = 0$ and only the region to the right of the mirror is considered. The vertical line corresponds to the spatial point $r = 0$ inside the shell, and the wavy horizontal line corresponds to the singularity at $r = 0$ outside the shell.

$$\frac{\partial^2\phi}{\partial t^2} - \frac{\partial^2\phi}{\partial r^2} = 0. \tag{3.2}$$

The general solution is of the form

$$\phi = g_F(u_F) + h_F(v), \tag{3.3}$$

where g_F and h_F are arbitrary functions. For the Schwarzschild metric (2.1),

$$\frac{\partial^2\phi}{\partial t^2} - \frac{\partial^2\phi}{\partial r_*^2} = 0, \tag{3.4}$$

which has a general solution of the form

$$\phi = g(u_i) + h(v), \tag{3.5}$$

where g and h are arbitrary functions. In the exterior region,

$$u_i = u_{\mathrm{ext}}, \tag{3.6}$$

and in the interior region,

$$u_i = u_{\mathrm{int}}. \tag{3.7}$$

A complete set of orthonormal mode functions that are solutions to Eq. (3.1) defines a "vacuum state" of the field ϕ. For the states we consider, each complete set can be broken up into separate sets of mode functions that we denote by f^i_ω with $\omega \geq 0$. Then

$$\phi = \int_0^\infty d\omega \sum_i [a^i_\omega f^i_\omega + a^{i\dagger}_\omega f^{i*}_\omega]. \tag{3.8}$$

The modes are normalized using the usual scalar product [7].

A. Boulware and Unruh states in Schwarzschild spacetime

The Boulware and Unruh states are composed of various combinations of two complete sets of modes: the Boulware modes and the Kruskal modes. We begin by discussing these two sets of modes. Our discussion will only focus on the behaviors of these modes in the interior and exterior regions. Because there is no scattering for the massless minimally coupled scalar field in two dimensions, we can write down analytic expressions for these modes everywhere in these regions.

The modes for the Boulware state are broken up into three subsets, those that have initial data given on the past horizon in the exterior region, which we denote by $h^{b\,\mathrm{ext}}_\omega$; those with initial data on the past horizon in the interior region, which are denoted by $h^{b\,\mathrm{int}}_\omega$; and those with initial data on past null infinity, which are denoted by $h^{\mathscr{I}^-}_\omega$. In the exterior region,

$$\begin{aligned} h^{b\,\mathrm{ext}}_\omega &= \frac{1}{\sqrt{4\pi\omega}} e^{-i\omega u_{\mathrm{ext}}}, \\ h^{b\,\mathrm{int}}_\omega &= 0, \\ h^{\mathscr{I}^-}_\omega &= \frac{1}{\sqrt{4\pi\omega}} e^{-i\omega v}. \end{aligned} \tag{3.9}$$

In the interior region,

$$\begin{aligned} h^{b\,\mathrm{ext}}_\omega &= 0, \\ h^{b\,\mathrm{int}}_\omega &= \frac{1}{\sqrt{4\pi\omega}} e^{-i\omega u_{\mathrm{int}}}, \\ h^{\mathscr{I}^-}_\omega &= \frac{1}{\sqrt{4\pi\omega}} e^{-i\omega v}. \end{aligned} \tag{3.10}$$

In [2], two states are actually discussed for the Unruh state. Both involve using the Boulware modes with initial data on past null infinity. One of the states involves using Kruskal modes that have initial data on the past horizon H^-. In the interior and exterior regions they have the form

$$p^b_\omega = \frac{1}{\sqrt{4\pi\omega}} e^{-i\omega U(u_i)}. \tag{3.11}$$

The other state involves using Boulware mode functions with initial data on the past horizon but with a different normalization so that in two dimensions in the region outside the horizon [29]

$$h^{\mathrm{th}}_\omega = \frac{e^{2\pi M\omega}}{\sqrt{2\sinh(4\pi M|\omega|)}} \frac{1}{\sqrt{4\pi|\omega|}} e^{-i\omega u_{\mathrm{ext}}}. \tag{3.12}$$

In this case the state includes both positive and negative values of ω. In many cases the two states give the same results for the vacuum expectation values of various quantities including the stress-energy tensor for the Unruh state in 2D. However, as was shown previously [28] for the symmetric two-point function they sometimes give very different results.

B. Vacuum state for the null shell spacetime

The natural *in* vacuum state for the massless minimally coupled scalar field in the null shell spacetime can be specified by requiring that on past null infinity

$$f_\omega^{\rm in} = \frac{e^{-i\omega v}}{\sqrt{4\pi\omega}} \tag{3.13}$$

and inside the shell at $r = 0$, the mode functions must vanish due to the existence of the perfectly reflecting mirror. These two conditions result in the following set of mode functions for the *in* state both inside and outside the null shell:

$$f_\omega^{\rm in} = \frac{1}{\sqrt{4\pi\omega}}(e^{-i\omega v} - e^{-i\omega u_F}). \tag{3.14}$$

Outside the null shell and the horizon $u_F = u_F(u_{\rm ext})$ is given by the relation (2.8). Outside the null shell and inside the horizon, $u_F = u_F(u_{\rm int})$ is given by the relation (2.10).

IV. SYMMETRIC TWO-POINT FUNCTION

The symmetric two-point correlation function for a scalar field is given by

$$G^{(1)}(x,x') \equiv \langle 0|[\phi(x)\phi(x') + \phi(x')\phi(x)]|0\rangle. \tag{4.1}$$

Substituting (3.8) into this equation gives

$$G^{(1)}(x,x') = \int_0^\infty d\omega \sum_i [f^i_\omega(x) f^{i*}_\omega(x') + f^i_\omega(x') f^{i*}_\omega(x)]. \tag{4.2}$$

For each of the sets of mode functions comprising the Boulware and Unruh, states, there is an infrared divergence of the form $\frac{1}{\omega}$ in the integrand, so we replace the lower limit with an infrared cutoff λ. For the Boulware state, in region I outside the horizon,

$$G^{(1)}_{\rm B\,ext}(x,x') = \int_\lambda^\infty d\omega \left[\frac{1}{4\pi\omega}\left(e^{-i\omega(u_{\rm ext}-u'_{\rm ext})} + e^{i\omega(u_{\rm ext}-u'_{\rm ext})} + e^{-i\omega(v-v')} + e^{i\omega(v-v')}\right)\right] \tag{4.3}$$

$$= -\frac{1}{2\pi}\{{\rm ci}[\lambda|u_{\rm ext} - u'_{\rm ext}|] - {\rm ci}[\lambda|v - v'|]\}. \tag{4.4}$$

In the interior region,

$$G^{(1)}_{B{\rm int}}(x,x') = \int_\lambda^\infty d\omega \left[\frac{1}{4\pi\omega}\left(e^{i\omega(u_{\rm int}-u'_{\rm int})} + e^{-i\omega(u_{\rm int}-u'_{\rm int})} + e^{i\omega(v-v')} + e^{-i\omega(v-v')}\right)\right] \tag{4.5}$$

$$= -\frac{1}{2\pi}\{{\rm ci}[\lambda|u_{\rm int} - u'_{\rm int}|] + {\rm ci}[\lambda|v - v'|]\}. \tag{4.6}$$

Here ci is the usual cosine integral function.

For the Unruh state there are two formulations of the mode functions, and they give very different results in this case. We will investigate this difference by focusing on the exterior region. It is easy to show that the first formulation (3.11) gives

$$\begin{aligned} G^{(1)}_{U-1}(x,x') &= -\frac{1}{2\pi}\Big\{{\rm ci}[\lambda|U(u_{\rm ext}) - U(u'_{\rm ext})|] + {\rm ci}[\lambda|v - v'|]\Big\} \\ &= \frac{1}{2\pi}\Big\{-{\rm ci}[4M\lambda e^{-u_{\rm ext}/4M}|1 - e^{(u_{\rm ext}-u'_{\rm ext})/4M}|] \\ &\quad - {\rm ci}[\lambda|v - v'|]\Big\}. \end{aligned} \tag{4.7}$$

Note that in the interior region one has the same expression with $u_{\rm ext} \to u_{\rm int}$.

The second formulation (3.12) requires two cutoffs near $\omega = 0$ in the integral from $-\infty < \omega < \infty$. Choosing them to be $\pm\lambda$ with $\lambda > 0$, one finds [29]

$$\begin{aligned} G^{(1)}_{U-2}(x,x') &= \frac{1}{2\pi}\int_\lambda^\infty \frac{d\omega}{\omega}\coth(4\pi M\omega)\cos[\omega(u_{\rm ext} - u'_{\rm ext})] \\ &\quad - \frac{1}{2\pi}{\rm ci}[\lambda|v - v'|]. \end{aligned} \tag{4.8}$$

The argument of the first cosine integral in (4.7) is proportional to $e^{-u_{\rm ext}/4M}$ and gets smaller as $u_{\rm ext}$ gets larger for fixed $u_{\rm ext} - u'_{\rm ext}$. We can use the expansion

$${\rm ci}(z) = \gamma_E + \log z + O(z^2), \tag{4.9}$$

where γ_E is Euler's constant, to obtain

$$\begin{aligned} G^{(1)}_{U-1}(x,x') = \frac{1}{2\pi}\Big\{&-\gamma_E + \frac{u_{\rm ext}}{4M} - \log[4M\lambda|1 - e^{(u_{\rm ext}-u'_{\rm ext})/4M|}] \\ &+ O(e^{-u_{\rm ext}/4M}) - {\rm ci}[\lambda|v - v'|]\Big\}. \end{aligned} \tag{4.10}$$

The approximation becomes better as $u_{\rm ext}$ increases and results in a linear growth of the two-point function in terms of $u_{\rm ext}$. This happens either as the future horizon is approached, or for fixed r, at late times when t is large. The latter is what was noted in [28]. For fixed $u_{\rm ext} - u'_{\rm ext}$, there is no such behavior in the second formulation (4.8).

To address the question of which formulation is the correct one in this case, note that the Unruh state was designed to mimic quantum effects in a black hole that forms from collapse at late times after the black hole forms. Thus, we can ask which formulation agrees with the late-time behavior of the symmetric two-point function for a black hole that forms from collapse. As shown in [28] for a particular splitting of the points, the first formulation of the Unruh state has this property for a black hole that forms from the collapse of a null shell in 2D. We generalize that argument here to an arbitrary splitting of the points, so long as they are on the same side of the horizon and outside the collapsing null shell.

For the *in* vacuum state for the collapsing null shell spacetime there is no infrared divergence. In this case it turns out to be easiest to compute $G^{(1)}$ using the same cutoff as in the previous calculations and then take the limit $\lambda \to 0$, using the relation (4.9). We find in the parts of the interior and exterior regions that are outside the null shell trajectory that

$$\begin{aligned} G^{(1)}_{\rm in}(x,x') &= \frac{1}{2\pi}\lim_{\lambda\to 0}\int_\lambda^\infty \frac{d\omega}{\omega}\Big\{\cos[\omega(v-v')] \\ &\quad + \cos[\omega(u_F(u_i)-u_F(u_i'))] \\ &\quad - \cos[\omega(u_F(u_i)-v')] - \cos[\omega(v-u_F(u_i'))]\Big\} \\ &= \frac{1}{2\pi}\log\left|\frac{(u_F(u_i)-v')(v-u_F(u_i'))}{(v-v')(u_F(u_i)-u_F(u_i'))}\right|, \end{aligned} \tag{4.11}$$

where $u_i = u_{\rm ext}$ in the exterior region and $u_i = u_{\rm int}$ in the interior region.

For large positive values of $u_{\rm ext}$, (2.8) gives

$$u_F(u_{\rm ext}) \approx v_H - 4Me^{(v_H-u_{\rm ext})/4M}. \tag{4.12}$$

Then to leading order one finds for large $u_{\rm ext}$ and fixed $u_{\rm ext}-u'_{\rm ext}$ that

$$G^{(1)}_{\rm in}(x,x') \to \frac{u_{\rm ext}}{8\pi M}, \tag{4.13}$$

which is the same leading order behavior as for $G^{(1)}_{U-1}$ in (4.10). Thus the first formulation of the Unruh state agrees with the large $u_{\rm ext}$ result for a black hole that forms from the collapse of a null shell, and the second formulation does not. Because of this, we shall only use the first formulation in what follows.

V. VACUUM POLARIZATION

The formal relation between the vacuum polarization and the symmetric two-point function is

$$\langle\phi^2(x)\rangle = \frac{1}{2}\lim_{x'\to x} G^{(1)}(x,x'). \tag{5.1}$$

However, there is a divergence when the two points come together, and thus this quantity has to be renormalized. Here, we use the method of point splitting. The point splitting counterterm in the 2D case is given in [32]. In general, renormalization counterterms do not depend on the state but do depend on how the points are split. Here, we assume that the points are split in the t direction in both the interior and the exterior regions. In the Appendix we show that the point splitting counterterms in this case are

$$\langle\phi^2\rangle_{ps} = -\frac{1}{2\pi}\left\{\gamma_E + \frac{1}{2}\log\left[\frac{|r-2M|\mu^2(t-t')^2}{4r}\right]\right\}, \tag{5.2}$$

where γ_E is Euler's constant and μ is an arbitrary constant with units of mass.[1] Then the renormalized expression is given by

$$\langle\phi^2\rangle = \lim_{t'\to t}\left[\frac{1}{2}G^{(1)}(t,r;t',r) - \langle\phi^2\rangle_{ps}\right]. \tag{5.3}$$

For the Boulware state, we use (4.9) to obtain

$$\langle\phi(x)^2\rangle_B = \frac{1}{4\pi}\log\left(\frac{|r-2M|}{4r}\frac{\mu^2}{\lambda^2}\right) \tag{5.4}$$

for both the interior and exterior regions.[2]

For differences of the Kruskal modes, the expansion in powers of $t-t'$ when $r'=r$ is more subtle. Since the renormalization counterterms are expanded in terms of $t-t'$, it is necessary to have the same expansions for the unrenormalized expressions. Using Taylor series expansions, one finds

$$\begin{aligned} U(u'_{\rm ext}) &\approx U(u_{\rm ext}) + \left(\frac{dU}{du_{\rm ext}}\right)(u'_{\rm ext}-u_{\rm ext}) \\ &= U(u_{\rm ext}) - e^{-\frac{u_{\rm ext}}{4M}}(t-t'), \end{aligned} \tag{5.5a}$$

$$\begin{aligned} U(u'_{\rm int}) &\approx U(u_{\rm int}) + \left(\frac{dU}{du_{\rm int}}\right)(u'_{\rm int}-u_{\rm int}) \\ &= U(u_{\rm int}) + e^{\frac{u_{\rm int}}{4M}}(t-t'), \end{aligned} \tag{5.5b}$$

[1]The existence of such an arbitrary constant in the renormalization counterterms for the vacuum polarization occurs for a massless scalar field with arbitrary curvature coupling in any 2D spacetime. This can be seen from the point splitting counterterms for a massive scalar field which contain a term that goes like $\log \frac{1}{2}m^2\sigma$ with a coefficient that does not go to zero in the massless limit [32]. For such a term one chooses an arbitrary mass scale μ when taking the massless limit. The same type of term appears in the 4D vacuum polarization counterterms in spacetimes where the scalar curvature R is nonzero [33]. For any spacetime that is not flat in 4D, there exist one or two arbitrary constants in the renormalization counterterms for any massless scalar field with nonconformal coupling to the scalar curvature. These constants provide finite renormalizations to coefficients of higher derivative terms in the gravitational Lagrangian [34].

[2]Note that the infrared cutoff in this case can, without loss of generality, be absorbed into the arbitrary mass scale μ.

$$\begin{aligned} V(v') &\approx V(v) + \left(\frac{dV}{dv}\right)(v'-v) \\ &= V(v) - e^{\frac{v}{4M}}(t-t'). \end{aligned} \tag{5.5c}$$

Using these results in (4.7) and combining with (5.2), it is straightforward to show that

$$\begin{aligned} \langle\phi^2(x)\rangle_U &= \frac{1}{4\pi}\left[\frac{t-r_*}{4M} + \log\left(\frac{|r-2M|}{4r}\frac{\mu^2}{\lambda^2}\right)\right] \\ &= \frac{u_{\rm ext}}{16\pi M} + \langle\phi^2\rangle_B, \end{aligned} \tag{5.6}$$

which, except for the last equality for $\langle\phi^2\rangle_U$, is valid in both the interior and the exterior regions.

To renormalize $\langle\phi^2\rangle_{\rm in}$, we expand $\frac{1}{2}G^{(1)}_{(\rm in)}$ in powers of $t-t'$ using Taylor series expansions which require the computation of $\frac{du_F}{du_{\rm ext}}$ and $\frac{du_F}{du_{\rm int}}$. These can be obtained from (2.7) and (2.9) with the result

$$\frac{du_F}{du_{\rm ext}} = \frac{1}{\frac{du_{\rm ext}}{du_F}} = \left(\frac{v_H - u_F}{v_0 - u_F}\right), \tag{5.7}$$

$$\frac{du_F}{du_{\rm int}} = \frac{1}{\frac{du_{\rm int}}{du_F}} = \left(\frac{v_H - u_F}{u_F - v_0}\right). \tag{5.8}$$

After some calculation, we find that

$$\begin{aligned} \langle\phi^2(x)\rangle_{\rm in} &= \frac{1}{4\pi}\left(2\gamma_E + \log\left|\frac{(v_0 - u_F(u_i))}{(v_H - u_F(u_i))}\right| + \log\left|(u_F(u_i)-v)^2\mu^2\frac{(r-2M)}{4r}\right|\right) \\ &= \frac{1}{4\pi}\left(2\gamma_E + \log\left|\frac{(v_0 - u_F(u_i))}{(v_H - u_F(u_i))}\right| + \log\left[\lambda^2(u_F(u_i)-v)^2\right]\right) + \langle\phi^2(x)\rangle_B, \end{aligned} \tag{5.9}$$

where again $u_i = u_{\rm ext}$ in the exterior region and $u_i = u_{\rm int}$ in the interior region. Note that there is no infrared divergence in the integrand for $G^{(1)}(x,x')$ in this case, so no lower limit cutoff needs to be introduced. In the second line we have inserted a factor of this cutoff in order to show explicitly the relationship with $\langle\phi^2\rangle_B$. The full expression is independent of λ.

A. Behaviors of the vacuum polarization

1. Boulware state

From (5.4), it is clear that $\langle\phi^2\rangle_B$ is independent of t and vanishes in the limit $r\to\infty$ if $\mu^2 = 4\lambda^2$. As expected for the Boulware state, it diverges on the past and future horizons and at $r=0$.

2. Unruh state

The behavior of $\langle\phi^2\rangle_U$ is more complicated due to its dependence on $u_{\rm ext}$ and $u_{\rm int}$. One would expect for the Unruh state that it would be finite on both past and future null infinity and the future horizon. One would also expect it to diverge on the past horizon and at the singularity at $r=0$.

If one substitutes $v-2r_*$ for $t-r_*$ in the first line of (5.6), it can be seen that on the future horizon

$$(\langle\phi^2\rangle_U)_{H^+} = \frac{1}{4\pi}\left[\frac{v}{4M} - 1 + \log\left(\frac{\mu^2}{4\lambda^2}\right)\right]. \tag{5.10}$$

This is finite as expected except in the limits $v\to\pm\infty$. From (5.6) one sees that $\langle\phi^2\rangle_U$ is also finite at future null infinity except in the limits $u_{\rm ext}\to\pm\infty$. Because of its linear dependence on $u_{\rm ext}$, it diverges at past and future timelike infinity, spacelike infinity, and at past null infinity. As expected it also diverges at $r=0$.

3. In state

Not surprisingly, the behavior of the vacuum polarization for the *in* state in the region outside the null shell is more complex.

Recall that $u_{\rm ext}\to+\infty$, both on the future horizon and in the limit $t\to\infty$ for fixed r. For large $u_{\rm ext}$ and $v > v_H$,

$$\begin{aligned} &u_F \approx v_H - 4M\exp\left(\frac{v_H - u_{\rm ext}}{4M}\right), \\ &\langle\phi^2\rangle_{\rm in} \approx \langle\phi^2\rangle_U + \frac{\log[\lambda^2(v-v_H)^2]}{4\pi} + \frac{\gamma_E}{2\pi} - \frac{v_H}{16\pi M}. \end{aligned} \tag{5.11}$$

Thus $\langle\phi^2\rangle_{\rm in}$ is finite on the future horizon, except in the limit $v\to\infty$ where it has the same leading order divergence as $\langle\phi^2\rangle_U$. It also approaches, to leading order, $\langle\phi^2\rangle_U$ at large t for fixed r. In both cases there is a subleading logarithmic divergence that does not occur for $\langle\phi^2\rangle_U$.

At large r, $u_F\approx u_{\rm ext}$ and

$$\begin{aligned} \langle\phi^2\rangle_{\rm in} \approx &\frac{1}{4\pi}\left(2\gamma_E + \log\left|\frac{(v_0 - u_{\rm ext})}{(v_H - u_{\rm ext})}\right| + \log\left[\lambda^2(u_{\rm ext}-v)^2\right]\right) \\ &+ \langle\phi(x)^2\rangle_B. \end{aligned} \tag{5.12}$$

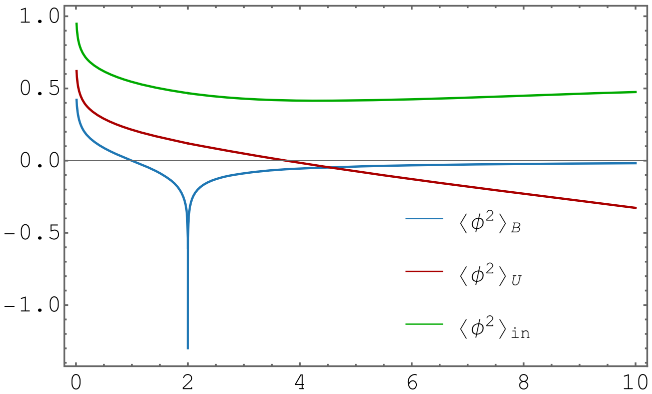

FIG. 3. Plot of $\langle\phi^2\rangle$ as a function of $\frac{r}{M}$. On the right-hand side of the plot, from top to bottom the curves are for the in (green), Boulware (blue), and Unruh (red) states. For the Unruh and *in* states, the plots are for the surface $\frac{v}{M} = 10$. For the Boulware and Unruh states $\frac{\mu}{\lambda}$ has been set to 1. For the *in* state, $\frac{\mu}{M}$ has been set to 1. Both the interior and the exterior regions are covered.

In this limit $\langle\phi^2\rangle_{\rm in}$ has very different behavior from $\langle\phi^2\rangle_U$ due to logarithmic divergences that occur whenever $r \to \infty$ and $v > v_0$.

In the interior, as the singularity is approached, $r_* \to 0$, and it is easy to see that outside of the null shell trajectory the divergence in $\langle\phi^2\rangle_{\rm in}$ is the same as that for $\langle\phi^2\rangle_B$. However, on the null shell trajectory $t = v_0 - r_*$ so $u_{\rm int} = 2r_* - v_0$ and $u_F(u_{\rm int}) = v_0 - 2r$ where the property $z = W(ze^z)$ has been used. Then one finds

$$(\langle\phi^2\rangle_{\rm in})_{v=v_0} = \frac{1}{4\pi}\left[2\gamma_E + 2\log\left(\frac{2r}{M}\right) + \log(M^2\mu^2)\right]. \tag{5.13}$$

Thus, there is a discontinuity in $\langle\phi^2\rangle_{\rm in}$ at the point where the null shell reaches $r = 0$ as can be seen by the fact that on the null shell trajectory as $r \to 0$, $\langle\phi^2\rangle_{\rm in} \sim \frac{1}{2\pi}\log(r/M)$ while $\langle\phi^2\rangle_B \sim -\frac{1}{4\pi}\log(r/M)$.

Some of these behaviors are illustrated in Figs. 3 and 4.

VI. STRESS-ENERGY TENSOR

As discussed in Sec. I, the stress-energy tensor for the massless minimally coupled scalar field has been computed previously for the states we are considering. The focus of previous analyses was the exterior region. In the Appendix, it is shown explicitly that the expressions obtained can be continued into the region inside the future horizon. In this section, we review their behaviors on the future horizon and analyze them in the interior region.

The stress-energy tensors can be written in terms of null coordinate components with the result [7][3]

$$\langle T_{uu}\rangle_B = \frac{1}{24\pi}\left[-\frac{M}{r^3} + \frac{3}{2}\frac{M^2}{r^4}\right], \tag{6.1a}$$

$$\langle T_{uu}\rangle_H = \langle T_{uu}\rangle_U = \frac{1}{768\pi M^2}\left(1-\frac{2M}{r}\right)^2\left[1+\frac{4M}{r}+\frac{12M^2}{r^2}\right] = \frac{1}{768\pi M^2} - \frac{M}{24\pi r^3} + \frac{M^2}{16\pi r^4}, \tag{6.1b}$$

$$\langle T_{uu}\rangle_{\rm in} = \frac{1}{24\pi}\left[-\frac{M}{r^3} + \frac{3}{2}\frac{M^2}{r^4} - \frac{8M}{(u_F(u_i)-v_0)^3} - \frac{24M^2}{(u_F(u_i)-v_0)^4}\right], \tag{6.1c}$$

$$\langle T_{vv}\rangle_B = \langle T_{uu}\rangle_B, \tag{6.1d}$$

$$\langle T_{vv}\rangle_H = \langle T_{uu}\rangle_H, \tag{6.1e}$$

$$\langle T_{vv}\rangle_U = \langle T_{vv}\rangle_{\rm in} = \langle T_{vv}\rangle_B, \tag{6.1f}$$

$$\langle T_{uv}\rangle_B = -\frac{1}{24\pi}\left(1-\frac{2M}{r}\right)\frac{M}{r^3}, \tag{6.1g}$$

$$\langle T_{uv}\rangle_H = \langle T_{uv}\rangle_U = \langle T_{uv}\rangle_{\rm in} = \langle T_{uv}\rangle_B. \tag{6.1h}$$

All of the above components for each of the four states diverge like r^{-4} as the singularity at $r = 0$ is approached. The coefficients differ in magnitude, but they all have the same positive sign.

As discussed in [7,35], for the stress energy to be regular on the event horizon one needs to go to a coordinate frame that is regular there. For Kruskal coordinates, one finds that for the stress energy to be finite on the future horizon, $(r-2M)^{-2}|\langle T_{uu}\rangle|$, $|(r-2M)^{-1}\langle T_{uv}\rangle|$, and $|\langle T_{vv}\rangle|$ should all be finite there. This is easily seen to be true for the Hartle-Hawking and Unruh states. As is well known, the stress-energy tensor for the Boulware state diverges on both the past and future horizons. For the *in* state, one can first make the substitution in (6.1c),

$$u_{\rm int} = r_* - t = 2r_* - v, \tag{6.2}$$

and note that v is continuous across the future horizon. Then, using a Taylor series expansion around $r = 2M$ with v held constant, one finds

$$\langle T_{uu}\rangle_{\rm in} \to \frac{(2M-r)^2}{512M^4\pi}\left[-1 + \exp\left(2 + \frac{v_H - v}{2M}\right)\right]. \tag{6.3}$$

Hence, the stress energy for the *in* state is finite at the horizon.

The flux of energy through the horizon is given by $\langle T_{vv}\rangle$. It is zero for the Hartle-Hawking state as expected. For the

[3]For completeness we include the stress-energy tensor for the Hartle-Hawking state here.

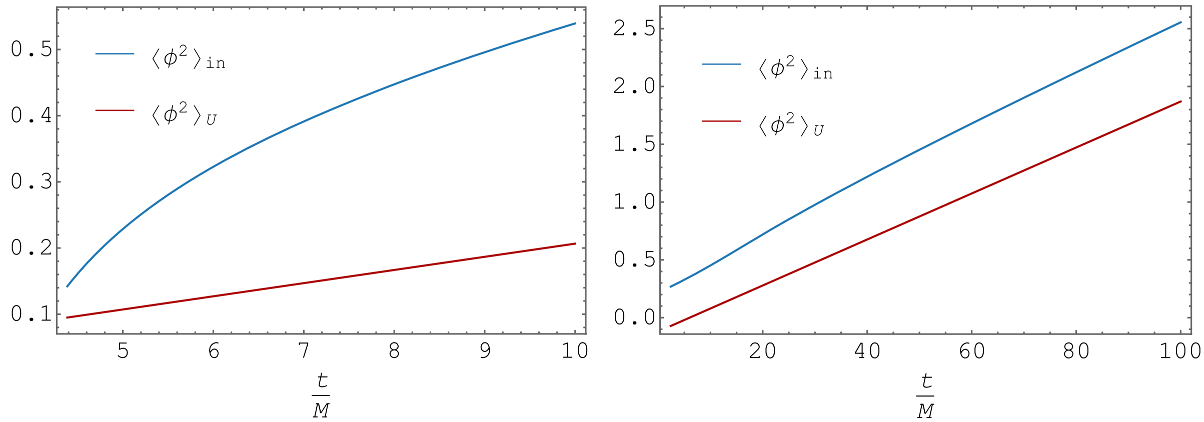

FIG. 4. Plots of $\langle\phi^2\rangle$ as a function of $\frac{t}{M}$. The upper (blue) curve corresponds to the *in* state with $v_0 = 4$ and the lower (red) curve corresponds to the Unruh state. For the Unruh state $\frac{\mu}{\lambda}$ has been set to 1, and for the *in* state $\frac{\mu}{M}$ has been set to 1. The left panel is for the interior region at $\frac{r}{M} = 1$ and the right panel is for the exterior region at $\frac{r}{M} = 3$. A careful examination shows that, as expected, $\langle\phi^2\rangle_{\rm in}$ is diverging faster than $\langle\phi^2\rangle_U$ in both regions.

Boulware, Unruh, and *in* states it is $\langle T_{vv}\rangle = -\frac{1}{768\pi M^2}$. As is well known, this is equal in magnitude and opposite in sign to the flux of energy $\langle T_{uu}\rangle$ reaching future null infinity at all times for the Unruh state and at late times for the *in* state. However, it is interesting to note that the same flux of negative energy goes through the future horizon in the Boulware state. It is also interesting to note that, even though $\langle T_{uu}\rangle_{\rm in}$ only approaches the value for the Unruh state asymptotically, $\langle T_{vv}\rangle_{\rm in}$ has the same value as for the Unruh state immediately after the null shell passes through the future horizon. There are no Einstein equations in 2D; however, if one had similar behavior in 4D, then one would expect that the spacetime geometry near the horizon, after the shell passes through it, would start to evolve in the same way that it would for the Unruh state. This is very different from how backreaction effects would manifest at large distances from the black hole. Of course in 4D there is an effective potential for the mode equation of the scalar field which would alter this picture due to backscattering of the outgoing modes through the future horizon.

The stress-energy tensor for the null shell spacetime is the only one of the four that we are considering which has a dependence on the coordinate t. The only component shown in (6.1) that is different from that of the Unruh state is $\langle T_{uu}\rangle_{\rm in}$. Since we are going to compare $\langle T_{uu}\rangle_{\rm in}$ with $\langle T_{uu}\rangle_U$, it is useful to plot the latter as a function of r. This is shown in Fig. 5.

As was done for $\langle\phi^2\rangle_{\rm in}$, using the identity for the Lambert W function, $z = W[ze^z]$, and the fact that on the null shell trajectory, $t = v_0 - r_*$, it is not hard to show that $\langle T_{uu}\rangle_{\rm in} = 0$ everywhere on the surface $v = v_0$. Therefore, it is discontinuous at the point where the null shell reaches $r = 0$.

In the exterior region one expects $\langle T_{uu}\rangle_U$ to be a good approximation to $\langle T_{uu}\rangle_{\rm in}$ at late times, and this is what is found [7]. However, it is not as clear what one would expect inside the future horizon, particularly since t is a space coordinate there.

Before exploring the details of how the Unruh state is approached, it is instructive to examine the behavior of this state which is shown in Fig. 5. There, one sees that this component decreases monotonically from its infinite value at $r = 0$ to zero at the future horizon. From there, it increases monotonically and approaches a constant value in the limit $r \to \infty$.

Some details as to how the Unruh state is approached are shown in Figs. 6 and 7. Note that the plots begin at the value of t for which the null shell passes through that value of r. For a fixed value of r in either the interior region or the exterior region, $\langle T_{uu}\rangle_{\rm in}$ approaches $\langle T_{uu}\rangle_U$ at large values of t. The smaller the value of r, the more "quickly" the approach occurs in both regions. In the exterior region, this means that the farther away one is from the horizon, the

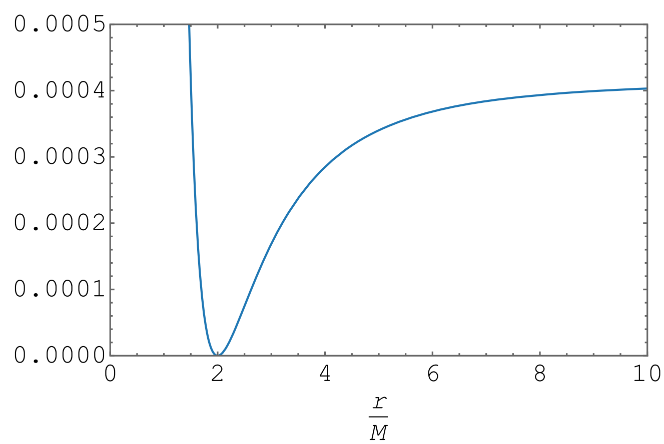

FIG. 5. Plot of $M^2\langle T_{uu}\rangle_U$ as a function of $\frac{r}{M}$. The plot covers both the interior and exterior regions. Note that $\langle T_{uu}\rangle_U$ diverges at $r = 0$, vanishes at $r = 2M$, and approaches a constant in the limit $r \to \infty$.

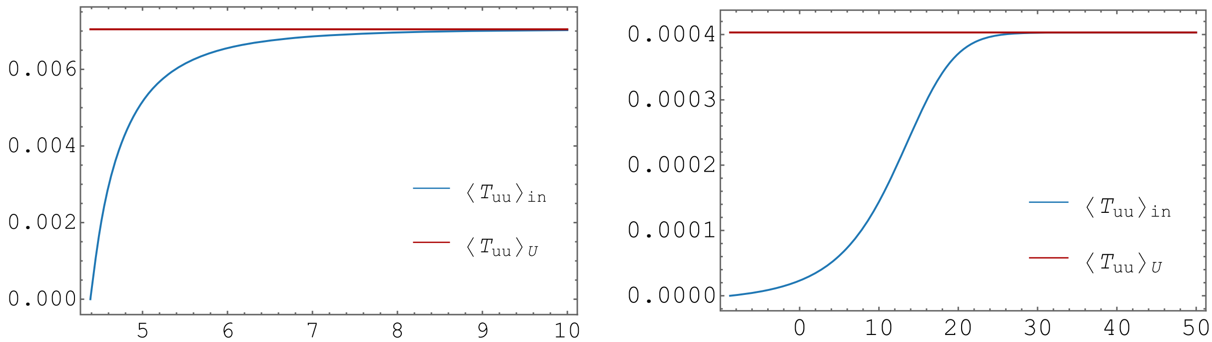

FIG. 6. $M^2\langle T_{uu}\rangle_{\rm in}$ is plotted as a function of $\frac{t}{M}$. For the panel on the left, this is done for the interior region for $\frac{r}{M}=1$, and for the panel on the right, it is done for the exterior region for $\frac{r}{M}=3$. The straight line on both plots is the value of $M^2\langle T_{uu}\rangle_U$.

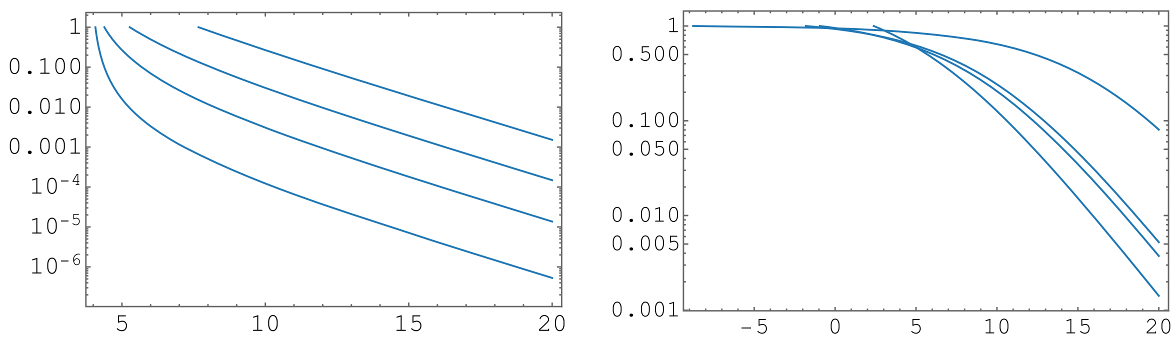

FIG. 7. The absolute value of the relative difference between $\langle T_{uu}\rangle_{\rm in}$ and $\langle T_{uu}\rangle_U$ is shown as a function of $\frac{t}{M}$. For the left panel, the curves from upper to lower correspond to $\frac{r}{M}=\frac{15}{8},\frac{3}{2}$, 1, and $\frac{1}{2}$. For the right panel, the curves from upper to lower on the right correspond to $\frac{r}{M}=10, 5, \frac{9}{2}$, and 3. Note that the curve for a given value of r, say $r=r_1$, begins at time $t_1=v_0-r_*(r_1)$, which is the time that the null shell reaches r_1. The smaller the value of r_1, the larger the value of t_1 in both the interior and exterior regions.

longer it takes for the stress energy to approach that of the Unruh state. In the interior region, it means that the closer one is in time $(-r)$ to the future horizon, the larger the region (in terms of the coordinate t) where the stress energy is significantly different from that for the Unruh state.

VII. CONCLUSIONS

We have computed the quantity $\langle\phi^2\rangle$ for a massless minimally coupled scalar field in Schwarzschild spacetime in 2D for the Boulware and Unruh states. We have also computed it for the *in* state when the field is in a 2D spacetime where a collapsing null shell forms a black hole. We have shown by explicit calculation, that for all of these states and the Hartle-Hawking state, previous calculations of the stress-energy tensor in the region outside the future horizon can be extendable to the region inside the future horizon.

The same type of late-time growth in $\langle\phi^2\rangle$ for the Unruh and *in* states was found in the exterior region as was previously found for the symmetric two-point function when the points are split in the radial direction [28]. This growth is linear for both states, and there is also logarithmic growth for the *in* state. This is important because it shows that the instability is not an artifact of the point separation. Similar growth in t occurs for fixed r and large values of t in the interior region.

For the Unruh state, $\langle\phi^2\rangle$ is also proportional to t at large negative values of t in both the interior and exterior regions. This is different from the symmetric two-point function. As $t\to-\infty$, one sees from (2.4b) that the Kruskal coordinates in the interior and exterior regions approach $\pm\infty$ respectively. Examination of (4.7) with the points split in the radial direction, shows that $G^{(1)}(x,x')\to-\frac{1}{2\pi}{\rm ci}(r_*-r'_*)$. Note that this limit does not exist for the null shell spacetime in either region. This result illustrates the fact that the two-point correlation function can give a very different answer in some cases than the quantity $\langle\phi^2\rangle$.

At the future horizon, $\langle\phi^2\rangle$ diverges for the Boulware state and is finite for the other states for finite values of v as expected. However, it does diverge in the limits $v\to\pm\infty$ for the Unruh state and in the limit $v\to+\infty$ for the *in* state which is a further indication of the instability of these states in 2D.

In the interior region, $\langle\phi^2\rangle$ diverges for all three states exactly in the same way as the singularity at $r=0$ is approached. For the Unruh state, there is a term proportional to t which is a spatial coordinate in the interior. For the *in* state, the dependence on t is more complicated. At fixed values of r there is both a term proportional to t and one proportional to $\log t$ at large values of t. The dependence on t indicates that the Unruh and *in* states are inhomogeneous in the interior.

The instabilities in $\langle\phi^2\rangle$ mentioned above in both the interior and exterior regions are not reflected in the 2D stress-energy tensors for the field. These stress-energy tensors have been previously studied in the exterior region and at the future horizon [7].

The stress energy for all four states diverges at the singularity as expected. As is well known, on the future horizon the only divergence in the stress energy is for the Boulware state.

The only state for which the stress energy has any dependence on t is the *in* state. In terms of null components, only $\langle T_{uu}\rangle$ has a dependence on t. This component vanishes on the null shell trajectory and increases outside of it. At fixed r for large values of t in both the interior and exterior regions, $\langle T_{uu}\rangle_{\rm in}$ approaches $\langle T_{uu}\rangle_U$.

The dependence of the stress energy on t in the interior region will occur for any black hole that forms from collapse in 2D or 4D. An important question is how well the Unruh state approximates quantum effects in the interior for a black hole in this case. This is because it is much easier in 4D to compute the stress-energy tensor for the Unruh state in the interior of an eternal black hole than it would be to compute it for one that forms from collapse. We find that, for fixed values of r as r gets smaller the range of values of t for which there is a significant difference from the stress tensor for the Unruh state decreases. At the same time, the spacetime curvature and the stress energy increase. If something similar happens in 4D, then back-reaction effects might be reasonably well approximated throughout much of the spacetime outside the collapsing matter by considering the Unruh state.

ACKNOWLEDGMENTS

We would like to thank Alessandro Fabbri and Ali Akil for helpful comments about the manuscript. P. R. A. would like to thank Northwestern's Center for Interdisciplinary Exploration and Research in Astrophysics (CIERA) for hosting him during a visit in August of 2023. This work was supported in part by the National Science Foundation under Grants No. PHY-1505875, No. PHY-1912584 and No. PHY-2309186 to Wake Forest University.

DATA AVAILABILITY

The data that support the findings of this article are openly available [36].

APPENDIX: STRESS-ENERGY TENSOR FOR A 2D SCHWARZSCHILD BLACK HOLE

In this Appendix, we derive an expression for the renormalized stress-energy tensor for a massless minimally coupled scalar field in a 2D black hole spacetime that works for the Boulware, Unruh, Hartle-Hawking, and *in* states and is valid in both the interior and exterior regions. We use the covariant point splitting method in [32]. This is equivalent to previous derivations using the Schwarzian derivative [7]. We explicitly show that the expressions for the stress-energy tensors for these states that were previously derived work for both the interior and exterior regions. At the end we also discuss the point splitting counterterms for $\langle\phi^2\rangle$.

A general expression for the unrenormalized stress-energy tensor for a massless minimally coupled scalar field and with the points split is of the form

$$\langle T_{\mu\nu}\rangle_{\rm unren} = \frac{1}{4}\left\{ g_\mu^{\alpha'} G^{(1)}_{;\alpha'\nu} + g_\nu^{\alpha'} G^{(1)}_{\mu\alpha'} - g_{\mu\nu} g^{\sigma\alpha'} G^{(1)}_{\sigma\alpha'} \right\}, \tag{A1}$$

where $G^{(1)}(x,x')$ is the symmetric two-point correlation function also called the Hadamard function. The bivector of parallel transport, $g_\mu^{\alpha'}$, is used to parallel transport vectors and tensors with primed indices from the point x' to the point x [33].

To go further, it is easiest to write the metric in the form

$$ds^2 = -f(r)dt^2 + \frac{dr^2}{f(r)}, \tag{A2}$$

where for Schwarzschild spacetime $f(r) = 1 - \frac{2M}{r}$. The main difference with the exterior region is that in the interior region $f < 0$, so t is a space coordinate and r is a time coordinate. To obtain an explicit expression, we separate the points x and x' in the t direction such that $x = (t, r)$ and $x' = (t', r)$ with $t - t' = \epsilon$. To renormalize the stress-energy tensor, we first expand $\langle T_{\mu\nu}\rangle_{\rm unren}$ in powers of ϵ and then expand the covariant point splitting counterterms in powers of ϵ. Taking the difference between the two expressions and setting $\epsilon = 0$ gives the renormalized expression for the stress-energy tensor.

To carry out this procedure, it is first necessary to consider derivatives of the quantity $\sigma(x,x')$, which is one half of the square of the proper distance between the points x and x' along the shortest geodesic connecting them. It satisfies the relation

$$\sigma = \frac{1}{2}\sigma_\mu\sigma^\mu \tag{A3}$$

with σ_μ the covariant derivative with respect to x^μ, and σ^μ is the geodesic's tangent vector at x which points toward x'. There is no difference in the derivation of its expansion in powers of ϵ between the interior and exterior regions. In [21], the following expressions for σ^t and σ^r are given in powers of ϵ:

$$\sigma^t = \sigma^t(\epsilon, r) = \epsilon + \frac{f'^2}{24}\epsilon^3 + \mathcal{O}(\epsilon^5), \tag{A4a}$$

$$\sigma^r = \sigma^r(\epsilon, r) = -\frac{ff'}{4}\epsilon^2 + \mathcal{O}(\epsilon^4). \tag{A4b}$$

The bivector of parallel transport is a vector at both x and x'. Thus it satisfies the relation $g_\mu^{\alpha'} = g_{\mu\rho} g^{\rho\alpha'}$. Using this, one can write (A1) in the form

$$\langle T_{\mu\nu}\rangle_{\rm unren} = \frac{1}{2} g_{\mu\rho} g^{\rho\alpha'} G^{(1)}_{;\alpha'\nu} - \frac{1}{4} g_{\mu\nu} g^{\sigma\alpha'} G^{(1)}_{\sigma\alpha'}. \quad (A5)$$

One way to compute $g^{\rho\alpha'}$ is to define two suitable orthonormal frames at points x and x' and use the relations

$$g^{\mu\nu'} = \eta^{ab} e^\mu_a e^{\nu'}_b, \quad (A6)$$

where e^μ_a and $e^{\nu'}_b$ are the orthonormal basis vectors of tetrads at x and x' respectively. Following the method given in [17,21], we set e^μ_0 to be in the time direction and e^μ_1 to be in the space direction. In the interior, these are in the r and t directions respectively. The orthonormality relation is

$$\eta_{ab} = g_{\mu\nu} e^\mu_a e^\nu_b, \quad (A7)$$

with η_{ab} the usual Minkowski metric. Since the shortest geodesic from the point (t', r) to the point (t, r) is spacelike in the interior and since its tangent vector is σ^μ, we set $e^\mu_1 = N\sigma^\mu$. Then (A7) gives $N = (\sigma_\mu \sigma^\mu)^{-1/2}$. Since (A7) implies that e^μ_0 and e^μ_1 are orthogonal, we can use this property to find e^μ_0. The result is

$$e^t_1 = \frac{\sigma^t}{(\sigma_\alpha\sigma^\alpha)^{\frac{1}{2}}}, \qquad e^r_1 = \frac{\sigma^r}{(\sigma_\alpha\sigma^\alpha)^{\frac{1}{2}}}, \quad (A8a)$$

$$e^t_0 = \frac{1}{f}\frac{\sigma^r}{(\sigma_\alpha\sigma^\alpha)^{\frac{1}{2}}}, \qquad e^r_0 = f\frac{\sigma^t}{(\sigma_\alpha\sigma^\alpha)^{\frac{1}{2}}}. \quad (A8b)$$

Aside from the fact that we are working in 2D, there are two differences between this result and the exterior result derived in [17,21]. One is that for this result the normalization is $(\sigma_\mu\sigma^\mu)^{-1/2}$ rather than $(-\sigma_\mu\sigma^\mu)^{-1/2}$, which is its value in the exterior region. The other is the switching of the basis vectors so that e^μ_0 in the exterior region goes to e^μ_1 in the interior region and e^μ_1 in the exterior region goes to e^μ_0 in the interior region. The reason is simply that t is a space coordinate in the interior region and a time coordinate in the exterior one.

One can define a similar set of tetrad basis vectors at x':

$$e^{t'}_1 = \frac{\sigma^{t'}}{(\sigma_{\alpha'}\sigma^{\alpha'})^{\frac{1}{2}}}, \qquad e^{r'}_1 = \frac{\sigma^{r'}}{(\sigma_{\alpha'}\sigma^{\alpha'})^{\frac{1}{2}}}, \quad (A9a)$$

$$e^{t'}_0 = \frac{1}{f}\frac{\sigma^{r'}}{(\sigma_{\alpha'}\sigma^{\alpha'})^{\frac{1}{2}}}, \qquad e^{r'}_0 = f\frac{\sigma^{t'}}{(\sigma_{\alpha'}\sigma^{\alpha'})^{\frac{1}{2}}}. \quad (A9b)$$

It is now necessary to expand $\sigma^{\mu'}$ as a power series in $\epsilon' = -\epsilon$. The method is the same as for the expansion of σ^μ, so one can simply substitute ϵ' for ϵ in (A4a) and (A4b), and then let $\epsilon' = -\epsilon$ with the result

$$\sigma^{t'}(\epsilon', r) = -\sigma^t(\epsilon, r), \quad (A10a)$$

$$\sigma^{r'}(\epsilon', r) = \sigma^r(\epsilon, r), \quad (A10b)$$

$$[\sigma_{\alpha'}(\epsilon', r)\sigma^{\alpha'}(\epsilon', r)]^{\frac{1}{2}} = -[\sigma_\alpha(\epsilon, r)\sigma^\alpha(\epsilon, r)]^{\frac{1}{2}}. \quad (A10c)$$

Note that the expansion for $[\sigma_{\alpha'}(\epsilon', r)\sigma^{\alpha'}(\epsilon', r)]^{\frac{1}{2}}$ ends up being in odd powers of ϵ' which is why it has the opposite sign as $[\sigma_\alpha(\epsilon, r)\sigma^\alpha(\epsilon, r)]^{\frac{1}{2}}$.

Therefore, the components of the bitensor parallel transport take the following form:

$$g^{tt'} = \frac{1}{\sigma_\alpha\sigma^\alpha}\left[\frac{1}{f^2}(\sigma^r)^2 + (\sigma^t)^2\right] = -\frac{1}{f} - \frac{f'^2}{8f}\epsilon^2 + O(\epsilon^4), \quad (A11a)$$

$$g^{tr'} = -g^{rt'} = -\frac{2\sigma^r\sigma^t}{\sigma_\alpha\sigma^\alpha} = -\frac{f'}{2}\epsilon + O(\epsilon^3), \quad (A11b)$$

$$g^{rr'} = -\frac{1}{\sigma_\alpha\sigma^\alpha}\left[f^2(\sigma^t)^2 + (\sigma^r)^2\right] = f + \frac{ff'^2}{8}\epsilon^2 + O(\epsilon^4). \quad (A11c)$$

The result in powers of ϵ is exactly the same as for the exterior region given in [21].

For the Boulware, Hartle-Hawking, and Unruh states we can write the symmetric two-point function in the general form

$$G^{(1)}(x, x') = -\frac{1}{2\pi}\Big\{\mathrm{ci}[\lambda|\mathscr{U}(u_i) - \mathscr{U}(u_i')|] + \mathrm{ci}[\lambda|\mathscr{V}(v) - \mathscr{V}(v')|]\Big\}. \quad (A12)$$

For the Boulware state $U(u_i) = u_i$ and $V(v) = v$, for the Hartle-Hawking state $\mathscr{U} = U$ and $\mathscr{V} = V$, and for the Unruh state $\mathscr{U} = U$ and $\mathscr{V} = v$.

For the *in* state the two-point function can be written in the form

$$G^{(1)}(x, x') = -\frac{1}{2\pi}\{\mathrm{ci}[\lambda|\mathscr{U}(u_i) - \mathscr{U}(u_i')|] + \mathrm{ci}[\lambda|\mathscr{V}(v) - \mathscr{V}(v')|] - \{\mathrm{ci}[\lambda|\mathscr{U}(u_i) - \mathscr{V}(v')|] - \mathrm{ci}[\lambda|\mathscr{V}(v) - \mathscr{U}(u_i')|]\Big]\}, \quad (A13)$$

with $\mathscr{U} = u_F$ and $\mathscr{V} = v$. Note that the first two terms are the same as for the other states. It turns out that the contributions from the third and fourth terms to the stress-energy tensor cancel even though they contribute to $\langle\phi^2\rangle$. So in what follows, we will ignore these terms and just consider derivatives of the expression for $G^{(1)}(x,x')$ in (A12) for all four states.

We next give the general expansion in powers of ϵ for two derivatives of G. Note that $\frac{d}{dz}\mathrm{ci}(\lambda z) = \frac{\cos(\lambda z)}{z}$. Therefore after computing the first derivative we can set $\lambda = 0$ since there is no longer an infrared divergence. The derivatives of $G^{(1)}$ that contribute to the stress-energy tensor are

$$G^{(1)}_{,u_i u_i'}(x,x') = -\frac{1}{2\pi}\frac{\frac{d\mathscr{U}(u_i)}{du_i}\frac{d\mathscr{U}(u_i')}{du_i'}}{(\mathscr{U}(u_i)-\mathscr{U}(u_i'))^2}, \tag{A14a}$$

$$G^{(1)}_{,vv'}(x,x') = -\frac{1}{2\pi}\frac{\frac{d\mathscr{V}(v)}{dv}\frac{d\mathscr{V}(v')}{dv'}}{(\mathscr{V}(v)-\mathscr{V}(v'))^2}. \tag{A14b}$$

Next, one can expand $\mathscr{U}(u_i')$ and $\mathscr{V}(v')$ in power series with the result

$$\mathscr{U}(u_i') = \mathscr{U}(u_i) - \left(\frac{d\mathscr{U}(u_i)}{du_i}\right)(u_i - u_i') + \ldots, \tag{A15a}$$

$$\mathscr{V}(v') = \mathscr{V}(v) - \left(\frac{d\mathscr{V}(v)}{dv}\right)(v - v') + \ldots. \tag{A15b}$$

With the definition

$$\epsilon = t - t', \tag{A16}$$

one easily finds the relations

$$\begin{aligned} v - v' &= \epsilon, \\ u_{\mathrm{int}} - u'_{\mathrm{int}} &= -\epsilon, \\ u_{\mathrm{ext}} - u'_{\mathrm{ext}} &= \epsilon. \end{aligned} \tag{A17}$$

Then one finds

$$G^{(1)}_{,u_i u_i'}(x,x') = -\frac{1}{2\pi}\left[\frac{1}{\epsilon^2} - \frac{1}{4}\left(\frac{\frac{d^2\mathscr{U}(u_i)}{du_i^2}}{\frac{d\mathscr{U}(u_i)}{du_i}}\right)^2 + \frac{1}{6}\left(\frac{\frac{d^3\mathscr{U}(u_i)}{du_i^3}}{\frac{d\mathscr{U}(u_i)}{du_i}}\right)\right], \tag{A18}$$

$$G^{(1)}_{,vv'}(x,x') = -\frac{1}{2\pi}\left[\frac{1}{\epsilon^2} - \frac{1}{4}\left(\frac{\frac{d^2\mathscr{V}(v)}{dv^2}}{\frac{d\mathscr{V}(v)}{dv}}\right)^2 + \frac{1}{6}\left(\frac{\frac{d^3\mathscr{V}(v)}{dv^3}}{\frac{d\mathscr{V}(v)}{dv}}\right)\right]. \tag{A19}$$

For the Hartle-Hawking state $\mathscr{V}(v) = V(v) = 4Me^{\frac{v}{4M}}$ in both the interior and exterior regions. For the other three states, $\mathscr{V}(v) = v$. Thus, $G^{(1)}_{,vv'}(x,x')$ is the same function of v in both regions. For the Boulware state $\mathscr{U}(u_i) = u_i$, so $G^{(1)}_{,u_i u_i'}(x,x')$ is the same in both regions. For the other states it is necessary to compute $G^{(1)}_{,u_i u_i'}(x,x')$ separately in both regions. The results can be written in the general form

$$\begin{aligned} G^{(1)}_{,u_i u_i'}(x,x') &= -\frac{1}{2\pi\epsilon^2} + \mathscr{A}, \\ G^{(1)}_{,vv'}(x,x') &= -\frac{1}{2\pi\epsilon^2} + \mathscr{B}, \end{aligned} \tag{A20}$$

where $\mathscr{A}$ and $\mathscr{B}$ are state-dependent constants. For the states we consider and the notation that we use, the values of $\mathscr{A}$ and $\mathscr{B}$ for a given state are the same for both the interior and exterior regions. For the Boulware state

$$\mathscr{A}_B = \mathscr{B} = 0, \tag{A21}$$

for the Unruh state

$$\mathscr{A}_U = \frac{1}{384\pi M^2} \qquad \mathscr{B}_U = 0, \tag{A22}$$

for the Hartle-Hawking state

$$\mathscr{A}_H = \mathscr{B}_H = \frac{1}{384\pi M^2}, \tag{A23}$$

and for the *in* state

$$\begin{aligned} \mathscr{A}_{\mathrm{in}} &= -\frac{2M}{3\pi[u_F(u_i) - v_0]^3} - \frac{2M^2}{\pi[u_F(u_i) - v_0]^4}, \\ \mathscr{B}_{\mathrm{in}} &= 0. \end{aligned} \tag{A24}$$

When the points are split in the t direction, it is easy to show using the chain rule and the definitions of u_i and v that

$$G^{(1)}_{,tt'}(x,x') = G^{(1)}_{,u_i u_i'}(x,x') + G^{(1)}_{,vv'}(x,x'), \tag{A25a}$$

$$G^{(1)}_{,tr'}(x,x') = G^{(1)}_{,rt'}(x,x') = \frac{1}{f}\left[-G^{(1)}_{,u_i u_i'}(x,x') + G^{(1)}_{,vv'}(x,x')\right], \tag{A25b}$$

$$G^{(1)}_{,rr'}(x,x') = \frac{1}{f^2}[G^{(1)}_{,u_i u_i'}(x,x') + G^{(1)}_{,vv'}(x,x')] = \frac{1}{f^2}G^{(1)}_{,tt'}(x,x'), \tag{A25c}$$

where $f = 1 - \frac{2M}{r}$. By substitution of (A25a)–(A25c) and (A11a)–(A11c) into (A5), we find

$$\langle T_{tt}\rangle_{\mathrm{unren}} = f^2\langle T_{rr}\rangle_{\mathrm{unren}} = -\frac{1}{2\pi\epsilon^2} - \frac{f'^2}{16\pi} + \frac{1}{2}(\mathscr{A} + \mathscr{B}), \tag{A26a}$$

$$\langle T_{tr}\rangle_{\mathrm{unren}} = -\frac{f'}{4\pi f\epsilon} - \frac{1}{2f}(\mathscr{A} - \mathscr{B}) + O(\epsilon). \tag{A26b}$$

To renormalize $\langle T_{\mu\nu}\rangle_{\rm unren}$, we subtract the renormalization counterterms and let the points come together. The renormalization counterterms are computed from the DeWitt-Schwinger expansion of the symmetric two-point function. The result in 2D is [32]

$$\langle T_{\mu\nu}(x,x')\rangle_{\rm DS} = \frac{1}{2\pi}\left\{(\sigma_\beta\sigma^\beta)^{-1}\left(g_{\mu\nu} - 2\frac{\sigma_\mu\sigma_\nu}{\sigma_\alpha\sigma^\alpha}\right) - \frac{1}{12}R\frac{\sigma_\mu\sigma_\nu}{\sigma_\alpha\sigma^\alpha}\right\}, \tag{A27}$$

with $R = -f''$. Substituting (A4a) and (A4b) into (A27) and subtracting the result from (A26a) and (A26b) one finds for the renormalized components of the stress-energy tensor:

$$\langle T_{tt}\rangle = -\frac{f'^2}{96\pi} + \frac{ff''}{24\pi} + \frac{1}{2}(\mathscr{A} + \mathscr{B}), \tag{A28a}$$

$$\langle T_{tr}\rangle = -\frac{1}{2f}(\mathscr{A} - \mathscr{B}), \tag{A28b}$$

$$\langle T_{rr}\rangle = \frac{1}{f^2}\left[-\frac{f'^2}{96\pi} + \frac{1}{2}(\mathscr{A} + \mathscr{B})\right]. \tag{A28c}$$

Next we convert to the null coordinate components to obtain

$$\langle T_{uu}\rangle = \frac{1}{4}(\langle T_{tt}\rangle + f^2\langle T_{rr}\rangle) - \frac{1}{2}f\langle T_{tr}\rangle = -\frac{f'^2}{192\pi} + \frac{ff''}{96\pi} + \frac{\mathscr{A}}{2}, \tag{A29a}$$

$$\langle T_{uv}\rangle = \frac{1}{4}(\langle T_{tt}\rangle - f^2\langle T_{rr}\rangle) = \frac{ff''}{96\pi}, \tag{A29b}$$

$$\langle T_{vv}\rangle = \frac{1}{4}(\langle T_{tt}\rangle + f^2\langle T_{rr}\rangle) + \frac{1}{2}f\langle T_{tr}\rangle = -\frac{f'^2}{192\pi} + \frac{ff''}{96\pi} + \frac{\mathscr{B}}{2}. \tag{A29c}$$

Evaluating these in each of the four states gives the expressions in (6.1a)–(6.1h) which we have now shown to be valid in both the interior and exterior regions.

The quantity $\langle\phi^2\rangle$ also needs to be renormalized. For a massless minimally coupled scalar field, the renormalization counterterm in a general spacetime is given by [32]

$$\langle\phi^2\rangle_{ps} = \frac{1}{2}G^{(1)}(x,x')_{DS} = -\frac{1}{2\pi}\left[\gamma_E + \frac{1}{2}\ln\left(\frac{\mu^2|\sigma|}{2}\right)\right] + \mathcal{O}(\sigma). \tag{A30}$$

Using the expansion in (A4a) and (A4b) along with the relation $\sigma = \frac{1}{2}\sigma_\alpha\sigma^\alpha$ one finds the expression in (5.2).

[1] D. Boulware, Quantum field theory in Schwarzchild and Rindler spaces, Phys. Rev. D **11**, 1404 (1975).
[2] W. G. Unruh, Notes on black-hole evaporation, Phys. Rev. D **14**, 870 (1976).
[3] J. B. Hartle and S. W. Hawking, Path-integral derivation of black-hole radiance, Phys. Rev. D **13**, 2188 (1976).
[4] P. C. W. Davies, S. A. Fulling, and W. G. Unruh, Energy-momentum tensor near an evaporating black hole, Phys. Rev. D **13**, 2720 (1976).
[5] S. A. Fulling, Alternative vacuum states in static space-times with horizon, J. Phys. A **10**, 917 (1977).
[6] W. Hiscock, Models of evaporating black holes I., Phys. Rev. D **23**, 2813 (1981).
[7] See for example, A. Fabbri, and J. Navarro-Salas, *Modeling Black Hole Evaporation* (Imperial College Press, London, 2005), and references contained therein.
[8] R. Balbinot and A. Fabbri, Quantum correlations across the horizon in acoustic and gravitational black holes, Phys. Rev. D **105**, 045010 (2022).
[9] S. Chakraborty, S. Singh, and T. Padmanabhan, A quantum peek inside the black hole event horizon, J. High Energy Phys. 06 (2015) 192.
[10] M. S. Fawcett and B. F. Whiting, in *Quantum Structure of Space and Time*, Proceedings of the Nuffield Workshop, Imperial College, London, edited by M. J. Duff and C. J. Isham (Cambridge University Press, Cambridge, England, 1982).
[11] P. Candelas and K. W. Howard, Vacuum $\langle\phi^2\rangle$ in Schwarzschild spacetime, Phys. Rev. D **29**, 1618 (1984).
[12] P. R. Anderson, $\langle\phi^2\rangle$ for massive fields in Schwarzschild spacetime, Phys. Rev. D **39**, 3785 (1989).
[13] A. Levi and A. Ori, Pragmatic mode-sum regularization method for semiclassical black-hole spacetimes, Phys. Rev. D **91**, 104028 (2015).
[14] A. Levi and A. Ori, Mode-sum regularization of $\langle\phi^2\rangle$ in the angular-splitting method, Phys. Rev. D **94**, 044054 (2016).
[15] M. S. Fawcett, The energy-momentum tensor near a black hole, Commun. Math. Phys. **89**, 103 (1983).
[16] K. W. Howard and P. Candelas, Quantum stress tensor in Schwarzschild space-time, Phys. Rev. Lett. **53**, 403 (1984).
[17] K. Howard, Vacuum $\langle T_\mu^\nu\rangle$ in Schwarzschild spacetime, Phys. Rev. D **30**, 2532 (1984).
[18] B. P. Jensen, J. G. Mc Laughlin, and A. C. Ottewill, Renormalized electromagnetic stress tensor for an evaporating black hole, Phys. Rev. D **43**, 4142 (1991).

[19] B. P. Jensen, J. G. Mc Laughlin, and A. C. Ottewill, Anisotropy of the quantum thermal state in Schwarzschild space-time, Phys. Rev. D **45**, 3002 (1992).

[20] P. R. Anderson, W. A. Hiscock, and D. A. Samuel, Stress-energy tensor of quantized scalar fields in static black hole spacetimes, Phys. Rev. Lett. **70**, 1739 (1993).

[21] P. R. Anderson, W. A. Hiscock, and D. A. Samuel, Stress-energy tensor of quantized scalar fields in static spherically symmetric spacetimes, Phys. Rev. D **51**, 4337 (1995).

[22] P. R. Anderson, R. Balbinot, and A. Fabbri, Cutoff anti–de Sitter space/conformal-field-theory duality and the quest for braneworld black holes, Phys. Rev. Lett. **94**, 061301 (2005).

[23] A. Levi and A. Ori, Versatile method for renormalized stress-energy computation in black-hole spacetimes, Phys. Rev. Lett. **117**, 231101 (2016).

[24] P. Taylor, C. Breen, and A. Ottewill, A mode-sum prescription for the renormalized stress energy tensor on black hole spacetimes, Phys. Rev. D **106**, 065023 (2022).

[25] P. Candelas and B. P. Jensen, Feynman Green function inside a Schwarzschild black hole, Phys. Rev. D **33**, 1596 (1986).

[26] A. Lanir, A. Levi, and A. Ori, Mode-sum renormalization of for a quantum scalar field inside a Schwarzschild black hole, Phys. Rev. D **98**, 084017 (2018).

[27] A. Ori and N. Zilberman, Computation of the semiclassical outflux emerging from a collapsing spherical null shell, Phys. Rev. Lett. **135**, 021401 (2025).

[28] P. R. Anderson and J. Traschen, Horizons and correlation functions in 2D Schwarzchild-de Sitter spacetime, J. High Energy Phys. 01 (2022) 192.

[29] P. R. Anderson, S. Gholizadeh Siahmazgi, and Z. P. Scofield, Infrared effects and the Unruh state, Classical Quantum Gravity **40**, 135004 (2022).

[30] I. M. Newsome, S. Pla, and P. R. Anderson, Quantum effects in $3+1$ Schwarzschild-de Sitter spacetime: Properties of the Hadamard function, Phys. Rev. D **111**, L021702 (2025).

[31] M. Good, P. Anderson, and C. Evans, Mirror reflections of a black hole, Phys. Rev. D **94**, 065010 (2016).

[32] T. Bunch, S. M. Christensen, and S. A. Fulling, Massive quantum field theory in two-dimensional Robertson Walker space-time, Phys. Rev. D **18**, 4435 (1978).

[33] S. Christensen, Vacuum expectation value of the stress tensor in an arbitrary curved background: The covariant point-separation method, Phys. Rev. D **14**, 2490 (1976).

[34] N. D. Birrell and P. C. W. Davies, *Quantum Fields in Curved Space* (Cambridge University Press, Cambridge, England, 1982).

[35] S. M. Christensen and S. A. Fulling, Trace anomalies and the Hawking effect, Phys. Rev. D **15**, 2088 (1977).

[36] P. R. Anderson, A. Peake, and S. Gholizadeh Siahmazgi, WakeSpace Scholarship (2026), https://wakespace.lib.wfu.edu/handle/10339/112289.